Target-depth estimation in active sonar

Alexis Mours, Cornel Ioana, Jerome I. Mars, Nicolas Josso, Yves Doisy

Target-depth estimation in active sonar

Alexis Mours,[a] Cornel Ioana, and Jérôme I. Mars[b]
Univ. Grenoble Alpes, GIPSA-Lab, F-38000 Grenoble France, CNRS, Gipsa-Lab, F-38000 Grenoble France

Nicolas F. Josso and Yves Doisy[c]
Thales Underwater Systems, 525 route Dolines, 06901 Sophia-Antipolis, France

INTRODUCTION

In active sonar, the objectives are to detect, localize and classify an underwater target. Azimuth and range are often used in anti-submarine warfare to localize targets. The depth may also be used as the key tactical information for strategy purposes or as a good feature for target classification or discrimination. Two dimensional arrays as flank arrays, cylindrical arrays, and hull-mounted arrays have access to elevation angles. Even linear towed arrays can give some information about the elevation using the different conical bearings measured when multipath propagation arises. In the context of long ranges and summer Mediterranean sound-speed profile (SSP), this paper presents a new target-depth estimation method, which uses elevation and arrival time measures from one sonar ping in a multipath environment. This method is based on ray back-propagation with a probabilistic approach. This localization algorithm minimizes the mean-squared error of elevation angles at the receiver and arrival times between a model and measures. This method is tested through Monte-Carlo simulations of classic active sonar scenarios and using experimental data from a real reduced-scaled tank. In active sonar, acoustic waves can take the same path on the way back or another path, so ray path combinations can occur. Our localization method discusses also about this ray identification, or how these combined acoustic paths were managed.

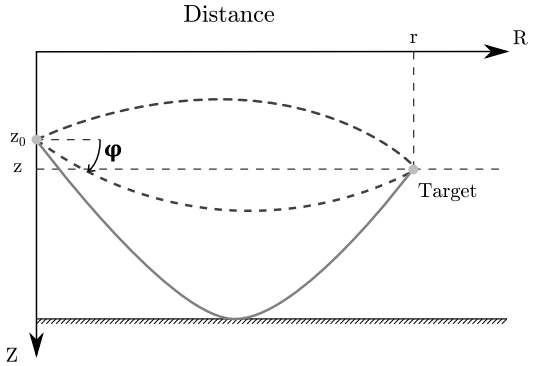

FIG. 1. Geometric conventions for sonar and target position, and for eigenrays. Example with two refracted rays and one bottom-reflected ray. φ is the ray angle at the receiver.

I. PROBLEM STATEMENT

This section introduces the problem of a target localization in active sonar. Consider a sonar system composed of an acoustic source and a receiver array that are co-located at $(R = 0, Z = z_0)$ in a water column as illustrated in Figure 1. The target is defined by the vector of random variables $\boldsymbol{X} = [r, z]^t$. Suppose that the azimuth of our own ship and the target are known and that the receiver array is able to compute elevation beamforming in the right bearing. We assume that one sonar ping was emitted from the sonar of our own ship, reflected by the target, and then finally recorded by the receiver array. Suppose that after all the signal-processing steps (*i.e.*, beamforming, matched filter, normalization and detection), there are N detected wavefronts. Let $\boldsymbol{\varphi}^{(m)}$ and $\boldsymbol{\tau}^{(m)}$ be the vectors of measure of the elevation angle and the wave travel time. The model of the measures is defined as follows:

$$\begin{aligned} \boldsymbol{\varphi}^{(m)} &= \boldsymbol{\varphi} + \boldsymbol{\delta\varphi} \\ \boldsymbol{\tau}^{(m)} &= \boldsymbol{\tau} + \boldsymbol{\delta\tau} \end{aligned} \tag{1}$$

where $\boldsymbol{\varphi} = [\varphi_1, .., \varphi_N]^t$ are the elevation angles, $\boldsymbol{\tau} = [\tau_1, .., \tau_N]^t$ are the two-way travel times, $\boldsymbol{\delta\varphi}$ and $\boldsymbol{\delta\tau}$ are vectors of independent zero-mean Gaussian noise with known standard deviations $\boldsymbol{\sigma_\varphi}$, $\boldsymbol{\sigma_\tau}$, and $.^t$ is the transpose operator. The sonar and the target are linked by eigenrays that represent acoustic paths taken by the sound wave to go from a point A to a point B. Contrary to passive sonar, acoustic waves in active sonar come back to the sonar after their reflection on the target. Acoustic waves can take the same path on the way back or another path, so ray path combinations can occur. Our localization method needs only the return travel times $\boldsymbol{T}$ of detected acoustic waves, i.e the travel times between the target and the receiver array. Due to possible ray path combinations, these variables are not obtainable without an assumption. So to simplify the problem, we assume that the return travel times $\boldsymbol{T}$ are estimated from the measurement of the two-way travel time $\boldsymbol{\tau}$ for only L detections. The subsection II.B explains how these are estimated.

[a] alexis.mours@gipsa-lab.grenoble-inp.fr
[b] jerome.mars@gipsa-lab.grenoble-inp.fr
[c] yves.doisy@fr.thalesgroup.com

II. TARGET LOCALIZATION

A. Semi-active localization

Our target localization algorithm is based on rays back-propagation taking into account the uncertainties of the measure. The principle is to propagate the measurement uncertainties from the array position to the target in a propagation simulator, and to compute a target-position probability density function (or a misfit function between model and measures). The propagation simulator used is Bellhop[1]. The target is assumed to be a single highlight (point target) model to assure that the eigenrays between the sonar and the target are similar to those between the target and the array. If the target moves during the wave propagation, the target position will be different for each acoustic propagation path. We assume that the position of the moving target is the same for each acoustic path, so this hypothesis simplifies the problem of a moving target by considering it as a fixed target with Doppler. We assume that all the detections are correctly separated in time or in elevation (difference higher than σ_φ or σ_τ).

The probabilistic approach of the method is detailed here. The a posteriori probability density function (PDF) of the target position, $p\left(\boldsymbol{X} \mid \boldsymbol{\varphi}^{(m)}, \boldsymbol{T}^{(m)}\right)$, is the conditional PDF that the target is located at $\boldsymbol{X}$ given the vectors of measure $(\boldsymbol{\varphi}^{(m)}, \boldsymbol{T}^{(m)})$. Using the Bayes' rule, the a posteriori probability can be expressed as follows:

$$p\left(\boldsymbol{X} \mid \boldsymbol{\varphi}^{(m)}, \boldsymbol{T}^{(m)}\right) = \frac{p\left(\boldsymbol{\varphi}^{(m)}, \boldsymbol{T}^{(m)} \mid \boldsymbol{X}\right) p\left(\boldsymbol{X}\right)}{p\left(\boldsymbol{\varphi}^{(m)}, \boldsymbol{T}^{(m)}\right)} \quad (2)$$

where $p\left(\boldsymbol{X}\right)$ is called the a priori PDF and contains the a priori information about the target position, and $p\left(\boldsymbol{\varphi}^{(m)}, \boldsymbol{T}^{(m)}\right)$ is the marginal PDF of the measures. In geo-acoustic inversion, the marginal PDF is independent of $\boldsymbol{X}$ and is usually assumed to be a constant. The a priori PDF, $p(\boldsymbol{X} = [r, z])$, is taken uniform in range and depth. The preceding equation becomes:

$$p\left(\boldsymbol{X} \mid \boldsymbol{\varphi}^{(m)}, \boldsymbol{T}^{(m)}\right) \propto p\left(\boldsymbol{\varphi}^{(m)}, \boldsymbol{T}^{(m)} \mid \boldsymbol{X}\right) p\left(\boldsymbol{X}\right) \quad (3)$$

For a given SSP, a target position $\boldsymbol{X} = [r, z]$ can also be defined by the vectors of elevation and one-way delay of the eigenrays: $(\boldsymbol{\varphi}(\boldsymbol{X}), \boldsymbol{T}(\boldsymbol{X}))$. So the conditional PDF $p\left(\boldsymbol{\varphi}^{(m)}, \boldsymbol{T}^{(m)} \mid \boldsymbol{X}\right)$, also called the likelihood function, can be re-written with the eigenray properties as follows:

$$p\left(\boldsymbol{\varphi}^{(m)}, \boldsymbol{T}^{(m)} \mid \boldsymbol{X}\right) = p\left(\boldsymbol{\varphi}^{(m)}, \boldsymbol{T}^{(m)} \mid \boldsymbol{\varphi}(\boldsymbol{X}), \boldsymbol{T}(\boldsymbol{X})\right) \quad (4)$$

where $\boldsymbol{\varphi}(\boldsymbol{X})$ and $\boldsymbol{T}(\boldsymbol{X})$ are the elevation and delay vectors, respectively, of the eigenrays for the target position $\boldsymbol{X}$. Assuming that each variables are all independent of each other, Equation (4) becomes:

$$p\left(\boldsymbol{\varphi}^{(m)}, \boldsymbol{T}^{(m)} \mid \boldsymbol{X}\right) = p\left(\boldsymbol{\varphi}^{(m)} \mid \boldsymbol{\varphi}(\boldsymbol{X})\right) p\left(\boldsymbol{T}^{(m)} \mid \boldsymbol{T}(\boldsymbol{X})\right) \quad (5)$$

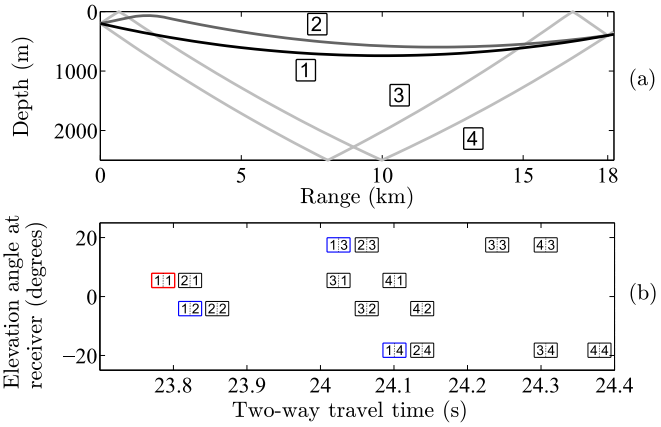

FIG. 2. (a) Example of propagation with four eigenrays between a sonar at 200 m in depth and a target at 400 m in depth and 18-km range. (b) Elevation angles at the receiver as a function of the two-way travel time for the two-way ray propagation of the top panel. In each box, the number of the left represents the ray path used between the sonar and the target, and the number of the right represents the ray path used between the target and the receiver array.

Finally the a posteriori PDF can be expressed as follows:

$$p\left(\boldsymbol{X} \mid \boldsymbol{\varphi}^{(m)}, \boldsymbol{T}^{(m)}\right) \propto p\left(\boldsymbol{\varphi}^{(m)} \mid \boldsymbol{\varphi}(\boldsymbol{X})\right) p\left(\boldsymbol{T}^{(m)} \mid \boldsymbol{T}(\boldsymbol{X})\right) p\left(\boldsymbol{X}\right) \quad (6)$$

The optimal target-position are the ones that maximizes the a posteriori probability of measured data. Instead of maximizing the probability, we prefer to minimize the following misfit function $E(\boldsymbol{X})$ that is the logarithm of the a posteriori probability :

$$E(\boldsymbol{X}) = \frac{|\boldsymbol{\varphi}^{(m)} - \boldsymbol{\varphi}(\boldsymbol{X})|^2}{\boldsymbol{\sigma}_\varphi^2} + \frac{|\boldsymbol{T}^{(m)} - \boldsymbol{T}(\boldsymbol{X})|^2}{\boldsymbol{\sigma}_\tau^2} + \log(C) \quad (7)$$

where C is a constant.

B. Estimation of one-way return travel-times

The localization algorithm needs the one-way return travel times of at least one detection. Figure 2(a) illustrates the ray propagation for the sonar scenario described in detail in section III. In this example, four eigenrays are considered between the sonar and the target: one down-refracted ray (1), one top-refracted ray (2), and two bottom-reflected rays (3,4). Figure 2(b) shows the ray elevations at the receiver for several detections as a function of the two-way travel time for two-way ray propagation. Each box represent a detection with sufficient SNR. These boxes are characterized by their elevations at the receiver and their two-way travel times. In each box, the number of the left represents the ray path used between the sonar and the target, and the number of the right represents the ray path used between the target and the receiver array. To estimate the one-way return travel time of a detection, the two-way

path type has to be known. A two-way path is defined as 'simple' (same number in the box) if the acoustic wave took the same path going backward and forward, and in the opposite sense, a two-way path is defined as 'combined' (different number in the box) if the acoustic wave took different paths going backward and forward. So the one-way return travel time T of a detection is not necessarily half of the two-way travel time τ. As a first step, we assume that the detection with the shortest delay (red box), τ_1, came from a simple path. So the one-way return travel time of this first detection, T_1, can be computed as follows:

$$T_1 = \tau_1/2 \tag{8}$$

Secondly, we assume that all of the detections that arrive first for each elevation angle at the receiver come from combined paths (blue boxes). These come necessarily from the one-way path of the ray with the shortest one-way travel time. So the one-way return travel times of each of these detections can be computed as follows:

$$T_i = \tau_i - T_1, \text{ for } i = 2, L \tag{9}$$

where L is the number of detected elevations.

III. SIMULATION

In this section, the localization algorithm is tested through two Monte-Carlo simulations with 500 runs. For these Monte-Carlo simulations, the first three detections were considered. Different combination of these three detections has been tested in order to show the impact of the number of rays used for the localization and to show the information contribution of each ray. The parameters of the active sonar scenario are described here:

- The SSP under the ship corresponds to a classical summer Mediterranean SSP:

$$\begin{aligned}(c_1, z_1) &= (0 \quad m, 1531\, m/s)\\ (c_2, z_2) &= (100 \quad m, 1507\, m/s)\\ (c_3, z_3) &= (2500\, m, 1546\, m/s)\end{aligned}$$

- The sonar depth as $z_0 = 200$ m.

- The sonar code used is a linear frequency modulation signal with a time duration $T_e = 2$ s, a frequency band $B = 500$ Hz, and a center frequency $f_0 = 5$ kHz. These parameters give a time and speed resolution at -3 dB as follows[2]:

$$2\tau_{-3dB} = 2T_{-3dB} = 2 \times \frac{0.44}{B} = 1.8 \text{ ms} \tag{10}$$

- The height of the array is H = 1 m. The elevation angle resolution at -3 dB is[3]:

$$2\varphi_{-3dB} = \frac{50c}{f_0 H} = 15 \text{ degrees} \tag{11}$$

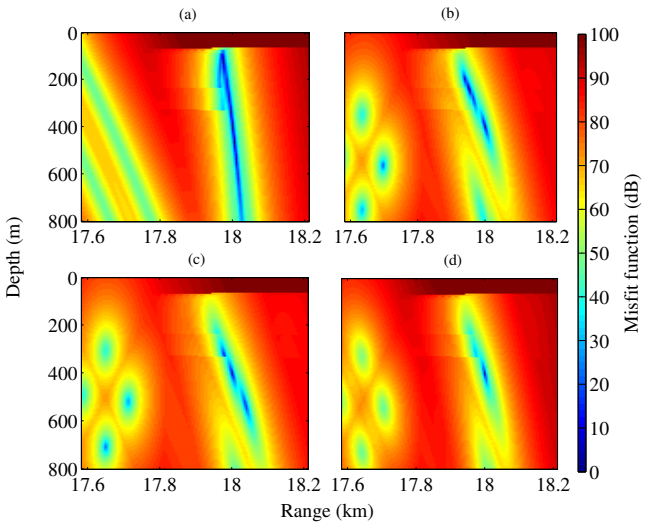

FIG. 3. Misfit functions for one run of the Monte-Carlo simulation. (a) Combination of (1|1) and (1|2). (a) Combination of (1|1) and (1|3). (a) Combination of (1|2) and (1|3). (a) Combination of (1|1), (1|2) and (1|3).

- The target range as $r = 18$ km and depth as $z = 400$ m.

For a point-like target, the standard deviations of T and φ can be expressed for large SNRs as follows[3]:

$$\sigma_{T_i} = \frac{T_{-3dB}}{\sqrt{SNR_{dB,i}}} \tag{12}$$

$$\sigma_{\varphi_i} = \frac{\varphi_{-3dB}}{\sqrt{SNR_{dB,i}}} \qquad \text{for } i = 1, .., L \tag{13}$$

where $SNR_{dB,i}$ is the SNR of the detection i at the array output. For a false alarm probability of 10^{-4} and a detection probability of 90%, a detection will be true if the SNR is above approximately 15 dB[4]. In the present paper, the SNR will be set to 15 dB for all true detections, and the time delay and elevation standard deviations are therefore 230 μs (35 cm) and 1.93 degrees, respectively. The first simulation proposes measures errors on elevations and arrival times that follows a normal distribution with standard deviations as σ_T and σ_φ. Figure 3 shows the misfit function in range and depth for one run and for the two-way path combination (1|1)+(1|2) (a), (1|1)+(1|3) (b), (1|2)+(1|3) (c) and (1|1)+(1|2)+(1|3) (d). The misfit function (d) with a combination of three detections is more accurate than a combination with two detections. So the estimation of the target-depth will be more robust with three detections in relation to the measure noise. The estimation of the target-depth with the combination of two detections is more difficult due to the presence of other minima in the misfit function ((b),(c)). In certain cases, these minima become lower than the minima corresponding to the true target position, and bias the target estimation. Figure 4 shows the histogram of the estimation of the target-depth for each rays combination. In Figure 4(a) and (b), there are some biased estimations of the target-depth due to the presence of other

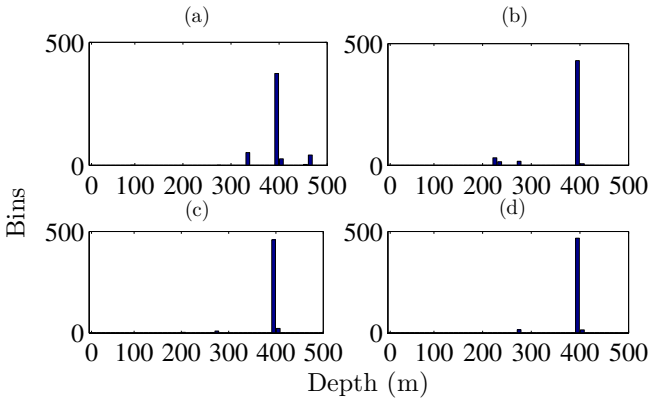

FIG. 4. First simulation. Histograms of the estimation of the target-depth of the Monte-Carlo simulation (500 runs) for four combinations of detections. (a) Combination of (1|1) and (1|2). (a) Combination of (1|1) and (1|3). (a) Combination of (1|2) and (1|3). (a) Combination of (1|1), (1|2) and (1|3).

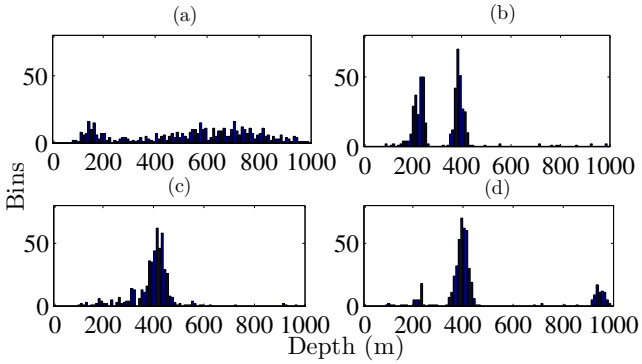

FIG. 5. Second simulation. Histograms of the estimation of the target-depth of the Monte-Carlo simulation (500 runs) for four combinations of ray. (a) Combination of (1|1) and (1|2). (a) Combination of (1|1) and (1|3). (a) Combination of (1|2) and (1|3). (a) Combination of (1|1), (1|2) and (1|3).

minima. The Figure 4(c) and (d) show an accurate and unbiased estimation of the target-depth, and therefore a robustness in relation to the measure noise. The errors on the elevation and time-delay measures are not preponderant compared to the errors of the environment variables. Errors in the sound-speed profile, sonar depth, bottom depth, and receiver tilt angle (environment inputs, generally) will probably cause larger bias and variance for the estimation of the target-depth. The robustness of the localization algorithm against SSP errors is then tested through this second Monte-Carlo simulation, by adding random SSPs to the previous simulation. The random SSP is generated by using empirical orthogonal functions (EOFs)[5,6]. These EOFs are extracted from an eigen decomposition of the covariance matrix from a database, which is a temporal historic of real SSPs for the months of July and August. The variability concerns only the upper layer of the SSP up to 100 m in depth with a maximum standard deviation of 4 m/s. The two-way path (1|1) will be the most affected by these random SSPs. Figure 5 shows the histogram of the estimation of the target-depth for each rays combination. The histogram in Figure 5(a) shows that the estimator of the target-depth is not robust in relation to the SSP errors. The histogram in Figure 5(b) shows that the estimator gives better result than the previous, but there is still a case (z=225m) where the estimator is strongly biased. The two other histograms in Figure. 5(c) and (d) show an unbiased estimator with a standard deviation of 100 m. The addition of a random SSP to the simulation shows that the target-position estimation and the associated standard deviation remain acceptable for three detections. It was also acceptable for two detections if they are coming from the bottom rather than from the surface, because there is less perturbation under the upper layer of the SSP. To go further, it would be interesting to simulate measures that take into account random bottom depth, array depth, or array tilt and to analyze the bias and the variance of each of these. If the bias are important due to environment parameter, the localization algorithm should include *a priori* on this random parameter in the process.

IV. EXPERIMENTAL DATA

This section proposes to validate our localization algorithm using experimental data from a real tank. An active sonar scenario in a shallow-water environment was reproduced in the experimental water tank of the ISTerre laboratory[7,8]. The dimensions of the water tank were 1.9 m x 0.9 m x 0.6 m. A scaling factor of 200:1 was used to model a 5-kHz active source in a deep ocean with a 0.7-m-diameter spherical target at a speed of 0.1 m/s. At a real scale, the metallic target would be immersed at 5.4 m depth, and the first hydrophone of the vertical uniform linear array would be at a depth of 4.8 m. The uniform linear array would be 112 m away from the target when the waveform is emitted. At the laboratory scale, the uniform linear array was composed of 64 half-wavelength-spaced transducers that had a 1-MHz carrier frequency and a 1-MHz bandwidth at -6 dB, with a sampling frequency of F_e = 20 MHz. The target that is a 3.5-mm spherical lead, was immersed at a depth of 37 mm and 550 mm away from the transducer. High waves of a few millimeters were generated on the surface layer to add random perturbation to the propagation. The experimental set-up is illustrated in Figure 6. The waveform was a binary phase-shift keying signal with a bandwidth of 600 kHz and a time duration of 500 μs. In this example, the elevation angle and the time resolution are φ_{-3dB} = 0.8 degree and τ_{-3dB} = 0.7 μs, respectively, the SSP was constant in depth, and the number of rays detected was four (*i.e.*, combination of the direct and the surface-reflected ray). Figure 7 shows the misfit function for one draw. It can be seen that no local minima appears in the misfit function. The true target depth was z_t = 37 mm ± 2 mm (at the real scale: z_t = 5.4 m ± 0.4 m) and the localization method provides

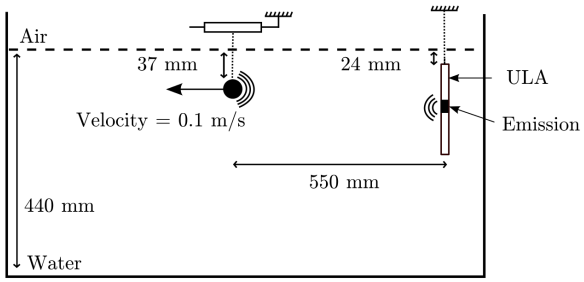

FIG. 6. Set-up of the experimental water-filled tank. The experiment was composed of a vertical uniform linear array (ULA) with 64 transducers, and a moving spherical target.

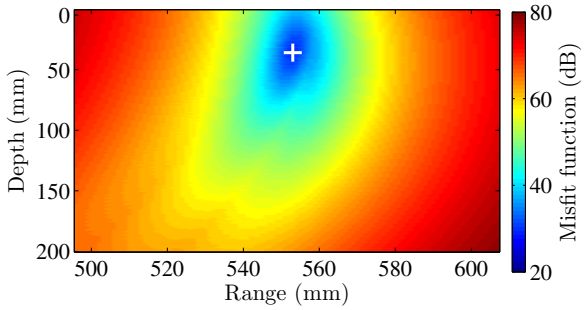

FIG. 7. Real data. Misfit function for one draw: $\hat{z}_t = 31.3$ mm (true target position: $z_t = 37$ mm $\pm$ 2 mm). The white crosshair represents the real target-position.

an expectation of the estimated target depth of $\mathrm{E}[\hat{z}_t] = 33.9$ mm $\pm$ 1.4 mm (at the real scale: $\mathrm{E}[\hat{z}_t] = 6.3$ m $\pm$ 0.3 m) over 10 realizations. The statistics of the target-depth estimation could be biased by the low number of realization, the array tilt, which was corrected but not measured, and the surface-reflected ray, which could be modified by the surface perturbations. At the real scale, the bias in target-depth estimation is only 1 m, so these results were adequate in order to validate our localization method with these experimental tank data.

V. CONCLUSIONS

Research in the target localization domain with an active sonar remains a poorly discussed topic. This paper focuses on estimation of the depth of a target using elevations and time-delay measures in active sonar and deep water, and especially for a summer Mediterranean SSP. The semi-active localization based on ray back-propagation and a probabilistic approach was tested for Monte-Carlo simulations and for water-tank experimental data. This method is also discussed in terms of ray identification and how the combined acoustic paths were managed. In others words, rays that have a different path from sonar to target and from target to array are taken into account. The simulation was realized for a target at 400 m in depth and 18-km range. The results suggest that the estimator of the target-depth was robust in relation to the measure noise and had a low standard deviation (1 m). The second simulation tries to analyze the influence of a random sound-speed profile. The results of this simulation suggests that the estimator of the target-depth was biased under certain choice of detections, but was robust using three detections for the algorithm. The standard deviation of the target-depth estimator obtained with three detections was near 100 m. However, some environmental parameters can still increase the bias and the variance of the target-depth estimator, such as random bottom depth, array depth, or array tilt. The results from the experimental data with surface noise reveal good estimation of the target depth and validate the localization algorithm for a constant SSP.

VI. ACKNOWLEDGMENTS

The author wishes to thank Philippe Roux for providing access and help to the experimental water tank of the ISTerre laboratory[7], and Xavier Cristol for many fruitful discussions.

REFERENCES

[1] M. B. Porter, "Bellhop gaussian beam/finite element beam code", Available in the Acoustics Toolbox, http://oalib.hlsresearch.com/Rays (2015).
[2] J.-P. Hermand and W. I. Roderick, "Delay-Doppler resolution performance of large time-bandwidth-product linear FM signals in a multipath ocean environment", J. Acoust. Soc. Am. **84**, 1709–1727 (1988).
[3] W. S. Burdic, *Underwater Acoustic Signal Analysis* (Prentice-Hall) (1984).
[4] G. Robertson, "Operating characteristics for a linear detector of cw in narrow-band gaussian noise", Bell System Technical Journal, The **46**, 755–774 (1967).
[5] L. R. LeBlanc and F. H. Middleton, "An underwater acoustic sound velocity data model", J. Acoust. Soc. Am. **67**, 2055–2062 (1980).
[6] W. Xu and H. Schmidt, "System-orthogonal functions for sound speed profile perturbation", IEEE J. Ocean. Engineering **31**, 156–169 (2006).
[7] P. Roux, I. Iturbe, B. Nicolas, J. Virieux, and J. I. Mars, "Travel-time tomography in shallow water: Experimental demonstration at an ultrasonic scale", J. Acoust. Soc. Am. **130**, 1232–1241 (2011).
[8] A. Mours, J. I. Mars, C. Ioana, N. F. Josso, Y. Doisy, and P. Roux, "Range, velocity and immersion estimation of a moving target in a water-filled tank with an active sonar system", in *OCEANS 2015-Genova*, 1–6 (IEEE) (2015).